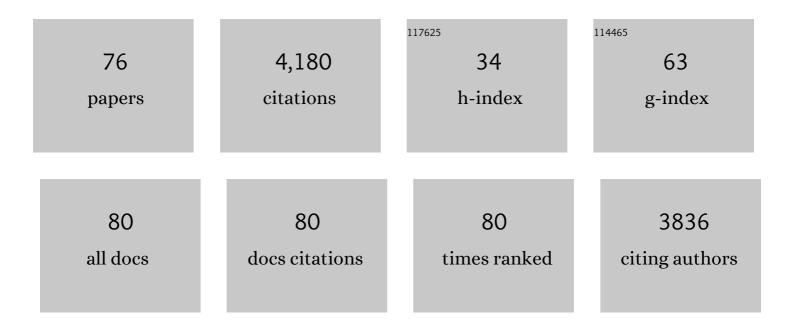
List of Publications by Year in descending order

Source: https://exaly.com/author-pdf/8149077/publications.pdf Version: 2024-02-01



#	Article	IF	CITATIONS
1	Probabilistic assessment of sea level during the last interglacial stage. Nature, 2009, 462, 863-867.	27.8	626
2	Spatiospectral Concentration on a Sphere. SIAM Review, 2006, 48, 504-536.	9.5	285
3	Localized spectral analysis on the sphere. Geophysical Journal International, 2005, 162, 655-675.	2.4	223
4	The deep structure of the Australian continent from surface wave tomography. Lithos, 1999, 48, 17-43.	1.4	207
5	Possible animal-body fossils in pre-Marinoan limestones from South Australia. Nature Geoscience, 2010, 3, 653-659.	12.9	180
6	Multimode Rayleigh wave inversion for heterogeneity and azimuthal anisotropy of the Australian upper mantle. Geophysical Journal International, 2002, 151, 738-754.	2.4	172
7	Accelerating changes in ice mass within Greenland, and the ice sheet's sensitivity to atmospheric forcing. Proceedings of the National Academy of Sciences of the United States of America, 2019, 116, 1934-1939.	7.1	152
8	lsostatic response of the Australian lithosphere: Estimation of effective elastic thickness and anisotropy using multitaper spectral analysis. Journal of Geophysical Research, 2000, 105, 19163-19184.	3.3	145
9	Spherical Slepian functions and the polar gap in geodesy. Geophysical Journal International, 2006, 166, 1039-1061.	2.4	129
10	Minimum-Variance Multitaper Spectral Estimation on the Sphere. Journal of Fourier Analysis and Applications, 2007, 13, 665-692.	1.0	124
11	A probabilistic assessment of sea level variations within the last interglacial stage. Geophysical Journal International, 2013, 193, 711-716.	2.4	96
12	Spectral estimation on a sphere in geophysics and cosmology. Geophysical Journal International, 2008, 174, 774-807.	2.4	92
13	Accelerated West Antarctic ice mass loss continues to outpace East Antarctic gains. Earth and Planetary Science Letters, 2015, 415, 134-141.	4.4	91
14	Multiscale adjoint waveform tomography for surface and body waves. Geophysics, 2015, 80, R281-R302.	2.6	91
15	Mapping Greenland's mass loss in space and time. Proceedings of the National Academy of Sciences of the United States of America, 2012, 109, 19934-19937.	7.1	87
16	Solving or resolving global tomographic models with spherical wavelets, and the scale and sparsity of seismic heterogeneity. Geophysical Journal International, 2011, 187, 969-988.	2.4	83
17	Seismic and mechanical anisotropy and the past and present deformation of the Australian lithosphere. Earth and Planetary Science Letters, 2003, 211, 271-286.	4.4	66
18	Spatiospectral localization of isostatic coherence anisotropy in Australia and its relation to seismic anisotropy: Implications for lithospheric deformation. Journal of Geophysical Research, 2003, 108, .	3.3	65

#	Article	IF	CITATIONS
19	Seismic constraints on temperature of the Australian uppermost mantle. Earth and Planetary Science Letters, 2005, 236, 227-237.	4.4	55
20	Automatic detection and rapid determination of earthquake magnitude by wavelet multiscale analysis of the primary arrival. Earth and Planetary Science Letters, 2006, 250, 214-223.	4.4	55
21	Age-dependent seismic thickness and mechanical strength of the Australian lithosphere. Geophysical Research Letters, 2002, 29, 24-1.	4.0	53
22	Coseismic and postseismic deformation of the 2011 Tohokuâ€Oki earthquake constrained by GRACE gravimetry. Geophysical Research Letters, 2012, 39, .	4.0	53
23	Ice mass loss in Greenland, the Gulf of Alaska, and the Canadian Archipelago: Seasonal cycles and decadal trends. Geophysical Research Letters, 2016, 43, 3150-3159.	4.0	53
24	Slepian Functions and Their Use in Signal Estimation and Spectral Analysis. , 2010, , 891-923.		52
25	Multiscale adjoint waveform-difference tomography using wavelets. Geophysics, 2014, 79, WA79-WA95.	2.6	49
26	Coseismic slip of the 2010 Mw 8.8 Great Maule, Chile, earthquake quantified by the inversion of GRACE observations. Earth and Planetary Science Letters, 2012, 335-336, 167-179.	4.4	48
27	Spatiospectral concentration in the Cartesian plane. GEM - International Journal on Geomathematics, 2011, 2, 1-36.	1.6	47
28	Quantitative characterization of coal by means of microfocal X-ray computed microtomography (CMT) and color image analysis (CIA). International Journal of Coal Geology, 1997, 34, 69-88.	5.0	46
29	Spatiospectral concentration of vector fields on a sphere. Applied and Computational Harmonic Analysis, 2014, 36, 1-22.	2.2	45
30	Spatiospectral localization of global geopotential fields from the Gravity Recovery and Climate Experiment (GRACE) reveals the coseismic gravity change owing to the 2004 Sumatraâ€Andaman earthquake. Journal of Geophysical Research, 2008, 113, .	3.3	44
31	Double-difference adjoint seismic tomography. Geophysical Journal International, 2016, 206, 1599-1618.	2.4	42
32	On the potential of recording earthquakes for global seismic tomography by low ost autonomous instruments in the oceans. Journal of Geophysical Research, 2009, 114, .	3.3	39
33	Seismic monitoring in the oceans by autonomous floats. Nature Communications, 2015, 6, 8027.	12.8	38
34	Global seismic tomography with sparsity constraints: Comparison with smoothing and damping regularization. Journal of Geophysical Research: Solid Earth, 2013, 118, 4887-4899.	3.4	35
35	Spectral and spatial decomposition of lithospheric magnetic field models using spherical Slepian functions. Geophysical Journal International, 2013, 193, 136-148.	2.4	35
36	Imaging the Galápagos mantle plume with an unconventional application of floating seismometers. Scientific Reports, 2019, 9, 1326.	3.3	33

#	Article	IF	CITATIONS
37	The origin of secondary microseism Love waves. Proceedings of the National Academy of Sciences of the United States of America, 2020, 117, 29504-29511.	7.1	27
38	Parametrizing surface wave tomographic models with harmonic spherical splines. Geophysical Journal International, 2008, 174, 617-628.	2.4	26
39	Efficient analysis and representation of geophysical processes using localized spherical basis functions. Proceedings of SPIE, 2009, , .	0.8	26
40	Highâ€resolution local magnetic field models for the Martian South Pole from Mars Global Surveyor data. Journal of Geophysical Research E: Planets, 2015, 120, 1543-1566.	3.6	24
41	Constraints on upper mantle viscosity from the flowâ€induced pressure gradient across the Australian continental keel. Geochemistry, Geophysics, Geosystems, 2010, 11, .	2.5	23
42	Wavelets and wavelet-like transforms on the sphere and their application to geophysical data inversion. Proceedings of SPIE, 2011, , .	0.8	23
43	Local spectral variability and the origin of the Martian crustal magnetic field. Geophysical Research Letters, 2012, 39, .	4.0	22
44	The spherical Slepian basis as a means to obtain spectral consistency between mean sea level and the geoid. Journal of Geodesy, 2012, 86, 609-628.	3.6	22
45	A future for drifting seismic networks. Eos, 2006, 87, 305.	0.1	20
46	A Suite of Software Analyzes Data on the Sphere. Eos, 2015, 96, .	0.1	18
47	Automatic discrimination of underwater acoustic signals generated by teleseismic P-waves: A probabilistic approach. Geophysical Research Letters, 2011, 38, n/a-n/a.	4.0	17
48	The exponentiated phase measurement, and objective-function hybridization for adjoint waveform tomography. Geophysical Journal International, 2020, 221, 1145-1164.	2.4	17
49	Maximum-likelihood estimation of lithospheric flexural rigidity, initial-loading fraction and load correlation, under isotropy. Geophysical Journal International, 2013, 193, 1300-1342.	2.4	16
50	How do we understand and visualize uncertainty?. The Leading Edge, 2006, 25, 542-546.	0.7	15
51	A spatiospectral localization approach to estimating potential fields on the surface of a sphere from noisy, incomplete data taken at satellite altitudes. Proceedings of SPIE, 2007, , .	0.8	13
52	Determining the Depth of Jupiter's Great Red Spot with Juno: A Slepian Approach. Astrophysical Journal Letters, 2019, 874, L24.	8.3	13
53	Generation of secondary microseism Love waves: effects of bathymetry, 3-D structure and source seasonality. Geophysical Journal International, 2021, 226, 192-219.	2.4	12
54	Internal and external potential-field estimation from regional vector data at varying satellite altitude. Geophysical Journal International, 0, , .	2.4	9

#	Article	IF	CITATIONS
55	Multiscale Estimation of Event Arrival Times and Their Uncertainties in Hydroacoustic Records from Autonomous Oceanic Floats. Bulletin of the Seismological Society of America, 2020, 110, 970-997.	2.3	9
56	Analysis of seafloor seismograms of the 2003 Tokachiâ€Oki earthquake sequence for earthquake early warning. Geophysical Research Letters, 2008, 35, .	4.0	8
57	A general approach to regularizing inverse problems with regional data using Slepian wavelets. Inverse Problems, 2017, 33, 125016.	2.0	8
58	A MERMAID Miscellany: Seismoacoustic Signals beyond the P Wave. Seismological Research Letters, 0, ,	1.9	7
59	Scalar and Vector Slepian Functions, Spherical Signal Estimation and Spectral Analysis. , 2015, , 2563-2608.		7
60	Robust surface-wave full-waveform inversion. , 2019, , .		6
61	Analysis of real vector fields on the sphere using Slepian functions. , 2012, , .		5
62	On the robustness of estimates of mechanical anisotropy in the continental lithosphere: A North American case study and global reanalysis. Earth and Planetary Science Letters, 2015, 419, 43-51.	4.4	5
63	The changing mass of glaciers on the Tibetan Plateau, 2002–2016, using time-variable gravity from the GRACE satellite mission. Journal of Geodetic Science, 2018, 8, 83-97.	1.0	5
64	Recording earthquakes for tomographic imaging of the mantle beneath the South Pacific by autonomous MERMAID floats. Geophysical Journal International, 2021, 228, 147-170.	2.4	5
65	One year of sound recorded by a <scp>mermaid</scp> float in the Pacific: hydroacoustic earthquake signals and infrasonic ambient noise. Geophysical Journal International, 2021, 228, 193-212.	2.4	5
66	A spatiospectral localization approach for analyzing and representing vector-valued functions on spherical surfaces. , 2013, , .		4
67	Mantle Transition Zone Receiver Functions for Bermuda: Automation, Quality Control, and Interpretation. Journal of Geophysical Research: Solid Earth, 2021, 126, e2020JB020177.	3.4	4
68	Potential-Field Estimation Using Scalar and Vector Slepian Functions at Satellite Altitude. , 2013, , 1-47.		4
69	Multi-physics adjoint modeling of Earth structure: combining gravimetric, seismic, and geodynamic inversions. GEM - International Journal on Geomathematics, 2020, 11, 1.	1.6	3
70	Instrument Response Removal and the 2020 MLgÂ3.1 Marlboro, New Jersey, Earthquake. Seismological Research Letters, 0, , .	1.9	3
71	Twenty-Thousand Leagues Under the Sea- Recording Earthquakes with Autonomous Floats. Acoustics Today, 0, 17, 42.	1.0	2
72	Potential-Field Estimation Using Scalar and Vector Slepian Functions at Satellite Altitude. , 2015, , 2003-2055.		2

#	Article	IF	CITATIONS
73	Full-waveform centroid moment tensor inversion of passive seismic data acquired at the reservoir scale. Geophysical Journal International, 2022, 230, 1725-1750.	2.4	2
74	Full-waveform adjoint tomography in a multiscale perspective. , 2014, , .		1
75	Scalar and Vector Slepian Functions, Spherical Signal Estimation and Spectral Analysis. , 2013, , 1-42.		1
76	Waveform inversion for shear velocity and attenuation via the spectral-element adjoint method. , 2021, , .		0